AIS Research Report No. 04-02

Architectural Information Systems Laboratory
Department of Architecture and Architectural Systems
Kyoto university
Sakyo, Kyoto 606-8501, Japan

Semidefinite Programming for Finite Element Analysis of Isotropic Materials with Unilateral Constitutive Laws

Y. Kanno[†] and M. Ohsaki[‡]

October 2004

Abstract A unified approach based on convex optimization is proposed for finding equilibrium configurations of structures consisting of no-tension or no-compression isotropic material in small strain and deformation. The semidefinite programming (SDP) problem is formulated so as to give the same optimizer as that of the minimization problem of total potential energy. An equilibrium configuration is obtained as an optimal solution of the SDP problem by using the primal-dual interior-point method. It is shown, in numerical examples, that equilibrium configurations are obtained without a priori knowledge of crack or wrinkling patterns.

Keywords: Masonry structure, No-tension material, Membrane, Semidefinite program, Interior-point method

[†] Dept. of Urban and Environmental Engineering, Kyoto Univ.
e-mail : kanno@archi.kyoto-u.ac.jp

[‡] Dept. of Architecture and Architectural Engineering, Kyoto Univ.
e-mail : ohsaki@archi.kyoto-u.ac.jp

1 Introduction

In many engineering applications, structural elements can be modeled not to transmit the tension forces. The so-called masonry structures [6] are typical examples, which may include ancient architectural heritage, brickwork walls, and concrete structures consisting of mortar, stones and/or bricks, etc. Among many models proposed for analyses of masonry structures [5, 10, 21], the assumption of *no-tension material* has been still widely used, and has received great attention [1, 6–8, 11, 20, 24]. In this paper, we restrict ourselves to the case in which no-tension material behaves as an elastic body which cannot transmit tension stresses, but otherwise behave as the linear elastic material. The stress–strain relation of this material is assumed to be reversible, i.e., there exists no energy dissipation. The microscopic model of no-tension material is that of a set of particles reacting elastically only through contact. In this paper, we assume that *masonry structures* consist only of no-tension material, and possibly have smeared cracks.

In quasi-static analyses of masonry structures, the constitutive law depends on the stress states, i.e., on the existence and directions of cracks. This is considered as the major difficulty of conventional methods, because trial-and-error processes are usually required in order to find the crack conditions which does not conflict with the incremental displacements. Therefore, it is desirable to develop a method based on a formulation irrespective of stress states. Under the assumption of plane-stress state and material isotropy, Giaquinta and Giusti [11] investigated the constitutive law of no-tension material. Maier and Nappi [20] formulated the same law as a linear complementarity condition by using a piecewise linear approximation of admissible stress set. A constitutive law of no-tension material under the thermal loads was presented by Padovani *et al.* [24]. Cuomo and Ventura [7] proposed a complementary energy formulation of no-tension material. Alfano *et al.* [1] performed numerical analyses of masonry structures based on a tangent-secant approach with the line search.

As the concept opposite to no-tension material, we may define *no-compression material*, which cannot transmit compression forces, but otherwise behave as the linear elastic material. We assume that a *membrane* is modeled as a two-dimensional structure which consists only of no-compression material, and may have smeared wrinkles. Lu *et al.* [19] proposed a numerical method for wrinkling membranes under the assumption of no-compression material. Pipkin [25] and Atai and Steigmann [3] formulated the strain energy function for membrane as a quasi-convexification of that for plate. The cables are regarded as the one-dimensional no-compression material. The authors proposed a second-order cone programming approach to find equilibrium configurations of cable networks [15].

In this paper, based on the convex optimization, we investigate the minimization problem of total potential energy for no-tension or no-compression structures, where

(i) we assume small strains and small rotations;

(ii) the structures consist only of no-tension or no-compression isotropic material;

(iii) smeared crack strain is assumed to be reversible and non-dissipative, hence our problems are path-independent [20].

In order to find equilibrium configurations of these structures, we propose novel formulations which are independent of the stress states, e.g., the existence and directions of cracks or wrinkles. It should be also noted that the formulation and implementation of the proposed methodology are quite independent of the fact that the problem is two- or three-dimensional.

Our approach in this paper is summarized as follows. We first formulate the minimization problem of total potential energy for no-tension continua as the (infinite-dimensional) optimization problem. Then we reformulate this problem into the *semidefinite programming* (*SDP*) problem [29] in the infinite-dimensional space. By applying the displacement-based finite-element discretization procedure, we show that the discretized version of the proposed problem is an SDP problem with the finite number of variables. An equilibrium configuration is obtained as an optimal solution of the proposed SDP problem by using the primal-dual interior-point method [18].

It is known that SDP can be solved efficiently by using the primal-dual interior-point method, where the number of arithmetic operations required is bounded by a polynomial of the size of problem [4, 18, 29]. Hence, by our method, equilibrium configurations of no-tension or no-compression structures are guaranteed to be obtained within the polynomial time of number of finite elements and number of degrees of freedom of the structure. The authors proposed efficient algorithms based on SDP for structural optimization with specified fundamental frequency [23] and linear buckling constraints [16].

This paper is organized as follows. In Section 2, we introduce SDP and its optimality conditions. In Section 3, we formulate the minimization problem of total potential energy for masonry structures or membranes. We show in Section 4 that the minimization problem of total potential energy can be reformulated into the (infinite-dimensional version of) SDP problem. Section 5 is devoted to the finite element discretization of the presented SDP problem. The resulting problem is also shown to be embedded into the (finite-dimensional) SDP problem. In Section 6, SDP problems are solved by using the primal-dual interior-point method in order to obtain equilibrium configurations of masonry structures and membranes.

2 Preliminary results

Throughout the paper, all vectors are assumed to be column vectors. However, for vectors $\boldsymbol{p} \in \mathbf{R}^n$ and $\boldsymbol{q} \in \mathbf{R}^m$, we often write

$$(\boldsymbol{p}, \boldsymbol{q}) = (\boldsymbol{p}^\top, \boldsymbol{q}^\top)^\top \in \mathbf{R}^{n+m}$$

in order to simplify the notation. The Cartesian product of two sets $\mathcal{U} \subseteq \mathbf{R}^n$ and $\mathcal{V} \subseteq \mathbf{R}^m$ is defined as

$$\mathcal{U} \times \mathcal{V} = \{(\boldsymbol{x}^\top, \boldsymbol{y}^\top)^\top | \boldsymbol{x} \in \mathcal{U},\ \boldsymbol{y} \in \mathcal{V}\}.$$

2.1 Matrices and Tensors

We write $\boldsymbol{p} \geq \boldsymbol{0}$ if a vector $\boldsymbol{p} = (p_i) \in \mathbf{R}^n$ satisfies $p_i \geq 0$ $(i = 1, \dots, n)$. Let $\mathcal{S}^n \subset \mathbf{R}^{n \times n}$ denote the set of all $n \times n$ real symmetric matrices. For $\boldsymbol{P} \in \mathcal{S}^n$ and $\boldsymbol{Q} \in \mathcal{S}^n$, we write $\boldsymbol{P} \succeq \boldsymbol{O}$ and $\boldsymbol{P} \succeq \boldsymbol{Q}$ if $\boldsymbol{P}$ and $\boldsymbol{P} - \boldsymbol{Q}$ are positive semidefinite, respectively.

In this paper, we often regard the vector $\boldsymbol{p} \in \mathbf{R}^n$ as the n-dimensional first-order tensor. The matrix $\boldsymbol{Q} \in \mathcal{S}^n$ is also regarded as the n-dimensional second-order symmetric tensor. For $\boldsymbol{Q} \in \mathcal{S}^n$, its eigenvalues, or its principal values, are denoted by q_i $(i = 1, \dots, n)$. We denote the inner products of $\boldsymbol{p}$, $\boldsymbol{q} \in \mathbf{R}^n$ and $\boldsymbol{P}$, $\boldsymbol{Q} \in \mathbf{R}^{n \times n}$, respectively, by

$$\boldsymbol{p}^\top \boldsymbol{q} = \sum_{i=1}^{n} p_i q_i,$$
$$\boldsymbol{P} \bullet \boldsymbol{Q} = \sum_{i=1}^{n} \sum_{j=1}^{n} P_{ij} Q_{ij} = \operatorname{tr}(\boldsymbol{P}^\top \boldsymbol{Q}).$$

However, in accordance with the conventional notations for tensors, we also write

$$\boldsymbol{p} \cdot \boldsymbol{q} = \boldsymbol{p}^\top \boldsymbol{q},$$
$$\boldsymbol{P} : \boldsymbol{Q} = \boldsymbol{P} \bullet \boldsymbol{Q}.$$

For $\boldsymbol{a} \in \mathbf{R}^n$ and $\boldsymbol{b} \in \mathbf{R}^n$, the tensor product $\boldsymbol{a} \otimes \boldsymbol{b}$ denotes an n-dimensional second-order tensor satisfying

$$(\boldsymbol{a} \otimes \boldsymbol{b}) \cdot \boldsymbol{c} = (\boldsymbol{b} \cdot \boldsymbol{c}) \boldsymbol{a}, \quad \forall \boldsymbol{c} \in \mathbf{R}^n.$$

Let $\boldsymbol{e}_i \in \mathbf{R}^n$ $(i = 1, \dots, n)$ denote the base vectors of reference frame $(x_1, \dots, x_n)$ in the n-dimensional space. Suppose that the vector field $\boldsymbol{b}(\boldsymbol{x}) \in \mathbf{R}^n$ is defined for the position vector $\boldsymbol{x} \in \mathbf{R}^n$. Then the gradient of $\boldsymbol{b}$ is written as

$$\boldsymbol{b} \otimes \nabla = \frac{\partial b_i}{\partial x_j} \boldsymbol{e}_i \otimes \boldsymbol{e}_j.$$

For given $\boldsymbol{A}_i \in \mathcal{S}^n$ $(i = 1, \dots, m)$, define the action of linear mapping $\mathcal{A} : \mathbf{R}^m \mapsto \mathcal{S}^n$ on $\boldsymbol{y} \in \mathbf{R}^m$ as [4]

$$\mathcal{A} \cdot \boldsymbol{y} = \sum_{i=1}^{m} \boldsymbol{A}_i y_i. \tag{1}$$

The adjoint operator $\mathcal{A}^* : \mathcal{S}^n \mapsto \mathbf{R}^m$ to $\mathcal{A}$ is defined as the linear operator satisfying $(\mathcal{A}^* : \boldsymbol{X}) \cdot \boldsymbol{y} = \boldsymbol{X} : (\mathcal{A} \cdot \boldsymbol{y})$ for any $\boldsymbol{X} \in \mathcal{S}^n$ and $\boldsymbol{y} \in \mathbf{R}^m$. From (1), we obtain

$$\mathcal{A}^* : \boldsymbol{X} = (\boldsymbol{A}_1 : \boldsymbol{X}, \dots, \boldsymbol{A}_m : \boldsymbol{X})^\top. \tag{2}$$

The **evec** operator is defined as stacking the columns of the lower triangle of $\boldsymbol{P} = (P_{ij}) \in \mathcal{S}^n$ on top of each other and multiplying the off-diagonal elements by 2, i.e.,

$$\mathbf{evec}(\boldsymbol{P}) = (P_{11}, 2P_{21}, \dots, 2P_{n1}, P_{22}, 2P_{32}, \dots, P_{nn})^\top \in \mathbf{R}^{n(n+1)/2}. \tag{3}$$

We denote the inverse map of **evec** by **Mat**, i.e., the implication

$$\boldsymbol{\pi} = \mathbf{evec}(\boldsymbol{P}) \quad \Longleftrightarrow \quad \boldsymbol{P} = \mathbf{Mat}(\boldsymbol{\pi})$$

holds for any $\boldsymbol{P} \in \mathcal{S}^n$ and $\boldsymbol{\pi} \in \mathbf{R}^{n(n+1)/2}$. It should be emphasized that the action of **Mat** on $\boldsymbol{\pi} \in \mathbf{R}^{n(n+1)/2}$ can be expressed in a form of

$$\mathbf{Mat}(\boldsymbol{\pi}) = \sum_{i=1}^{n(n+1)/2} \boldsymbol{I}_i \pi_i$$

by using the appropriate constant matrices $\boldsymbol{I}_i \in \mathcal{S}^n$. Consequently, with $\mathcal{A}_z : \mathbf{R}^k \mapsto \mathcal{S}^n$ and a constant matrix $\boldsymbol{D} \in \mathcal{S}^n$, the condition in the form of

$$\mathbf{Mat}(\boldsymbol{\pi}) + \mathcal{A}_z \cdot \boldsymbol{z} + \boldsymbol{D} \succeq \boldsymbol{O} \tag{4}$$

is regarded as the *linear matrix inequality* [4] in terms of $(\boldsymbol{\pi}, \boldsymbol{z}) \in \mathbf{R}^{n(n+1)/2} \times \mathbf{R}^k$.

The operator which transforms a symmetric matrix $\boldsymbol{P} \in \mathcal{S}^n$ into an $n(n+1)/2$-dimensional vector was used by Helmberg [12], Todd *et al.* [28]. They used the notation **svec**, and its definition is slightly different from **evec** introduced in (3). Indeed, by applying **svec**, the off-diagonal elements of $\boldsymbol{P} \in \mathcal{S}^n$ are multiplied by $\sqrt{2}$ instead of 2. However, we use **evec** in this paper, because $\mathbf{evec}(\boldsymbol{E})$ for a symmetric linear strain tensor $\boldsymbol{E}$ coincides with so-called *strain vector* with reordering its elements.

2.2 Semidefinite Program

The *semidefinite programming* (*SDP*) problem refers to the optimization problem having the form of [29]

$$\left.\begin{array}{ll} \min & \boldsymbol{C} : \boldsymbol{X} \\ \text{s.t.} & \mathcal{A}^* : \boldsymbol{X} = \boldsymbol{b}, \quad \mathcal{S}^n \ni \boldsymbol{X} \succeq \boldsymbol{O}, \end{array}\right\} \tag{5}$$

where $\boldsymbol{X}$ is variable, $\mathcal{A}$ is the linear operator defined by (1) for constant $\boldsymbol{A}_i \in \mathcal{S}^n$ $(i = 1, \dots, m)$, and $\boldsymbol{b} \in \mathbf{R}^m$ and $\boldsymbol{C} \in \mathcal{S}^n$ are constants. The dual of Problem (5) is formulated in variable $\boldsymbol{y} \in \mathbf{R}^m$ as

$$\left.\begin{array}{ll} \max & \boldsymbol{b} \cdot \boldsymbol{y} \\ \text{s.t.} & \boldsymbol{C} - \mathcal{A} \cdot \boldsymbol{y} \succeq \boldsymbol{O}. \end{array}\right\} \tag{6}$$

Observe that the dual SDP problem (6) is the minimization problem of linear function over the linear matrix inequality in terms of $\boldsymbol{y}$. Hence, the constraint in a form of (4) can be embedded into the constraint of SDP problem (6) by putting $\boldsymbol{y} = (\boldsymbol{\pi}, \boldsymbol{z})$.

Recently, SDP has received increasing attention for its wide fields of application [4, 23, 29]. It is well-known that *linear program* (*LP*), *second-order cone program* (*SOCP*), etc., are included by SDP as the special cases [4]. It is theoretically guaranteed that the primal-dual interior-point method [18] converges to the optimal solutions of the pair of SDP problems (5) and (6) within the number of arithmetic operations bounded by a polynomial of n and m [4, 18].

2.3 Optimality conditions of nonlinear SDP

Let $f : \mathcal{S}^n \mapsto \mathbf{R}$ and $\boldsymbol{G} : \mathcal{S}^n \mapsto \mathcal{S}^n$ be continuously differentiable functions. Consider the following optimization problem called the nonlinear SDP problem in variable $\boldsymbol{Z} \in \mathcal{S}^n$:

$$\left.\begin{array}{ll} \min & f(\boldsymbol{Z}) \\ \text{s.t.} & \boldsymbol{G}(\boldsymbol{Z}) \succeq \boldsymbol{O}. \end{array}\right\} \tag{7}$$

See, e.g., Kanzow *et al.* [17] and Jarre [13] for the optimality conditions of nonlinear SDP problems and optimization algorithms. However, the form of Problem (7) is slightly different from the problems dealt with in [13, 17].

Let $Df(\boldsymbol{Z}')$ and $D\boldsymbol{G}(\boldsymbol{Z}')$ denote the derivatives of the mapping $f(\cdot)$ and $\boldsymbol{G}(\cdot)$, respectively, at $\boldsymbol{Z}' = (Z'_{ij}) \in \mathcal{S}^n$ defined such that $Df(\boldsymbol{Z}') \bullet \boldsymbol{H}$ and $D\boldsymbol{G}(\boldsymbol{Z}') \bullet \boldsymbol{H}$ are linear functions of $\boldsymbol{H} \in \mathbf{R}^{n \times n}$ given by

$$\begin{aligned} Df(\boldsymbol{Z}') \bullet \boldsymbol{H} &= \sum_{i=1}^{n} \sum_{j=1}^{n} H_{ij} \left. \frac{\partial f(\boldsymbol{Z})}{\partial Z_{ij}} \right|_{\boldsymbol{Z}=\boldsymbol{Z}'}, \\ D\boldsymbol{G}(\boldsymbol{Z}') \bullet \boldsymbol{H} &= \sum_{i=1}^{n} \sum_{j=1}^{n} H_{ij} \left. \frac{\partial \boldsymbol{G}(\boldsymbol{Z})}{\partial Z_{ij}} \right|_{\boldsymbol{Z}=\boldsymbol{Z}'}. \end{aligned}$$

Let $\boldsymbol{W} \in \mathcal{S}^n$ be a Lagrange multiplier. The Lagrangian $L : \mathcal{S}^n \times \mathcal{S}^n \mapsto [-\infty, +\infty]$ of Problem (7) is formulated as

$$L(\boldsymbol{Z}, \boldsymbol{W}) = \begin{cases} f(\boldsymbol{Z}) - \boldsymbol{W} \bullet \boldsymbol{G}(\boldsymbol{Z}) & (\boldsymbol{W} \succeq \boldsymbol{O}), \\ +\infty & (\text{otherwise}). \end{cases} \tag{8}$$

Indeed, by using the self-duality of the cone $\{\boldsymbol{W} \in \mathcal{S}^n | \boldsymbol{W} \succeq \boldsymbol{O}\}$ [4], we see that Problem (7) is equivalent to

$$\min_{\boldsymbol{Z} \in \mathcal{S}^n} \quad \sup\{L(\boldsymbol{Z}, \boldsymbol{W}) | \boldsymbol{W} \in \mathcal{S}^n\},$$

which validates that L can be regarded as the Lagrangian of Problem (7) (see, e.g., [26, Theorem 36.5]). Then the optimality conditions are immediately obtained as follows:

Proposition 2.1. *Suppose that f and $\boldsymbol{G}$ are convex. $\boldsymbol{Z}$ is an optimal solution of the nonlinear SDP problem* (7) *if and only if there exists a $\boldsymbol{W} \in \mathcal{S}^n$ satisfying the Karush-Kuhn-Tucker (KKT) conditions*

$$Df(\boldsymbol{Z}) - \boldsymbol{W} \bullet D\boldsymbol{G}(\boldsymbol{Z}) = \boldsymbol{O}, \tag{9}$$

$$\boldsymbol{G}(\boldsymbol{Z}) \succeq \boldsymbol{O}, \quad \boldsymbol{W} \succeq \boldsymbol{O}, \quad \boldsymbol{G}(\boldsymbol{Z}) \bullet \boldsymbol{W} = 0. \tag{10}$$

Proof. Apply Theorem 36.6 in [26] to L defined by (8). □

As is well known, for $\boldsymbol{G} \succeq \boldsymbol{O}$ and $\boldsymbol{W} \succeq \boldsymbol{O}$, the condition $\boldsymbol{G} \bullet \boldsymbol{W} = 0$ is equivalent to [2]

$$\boldsymbol{G}\boldsymbol{W} = \boldsymbol{O}. \tag{11}$$

Moreover, the complementarity condition (11) is equivalent to the complementarity condition in terms of eigenvalues of $\boldsymbol{G}$ and $\boldsymbol{W}$ as follows:

Proposition 2.2. *$\boldsymbol{G} \in \mathcal{S}^n$ and $\boldsymbol{W} \in \mathcal{S}^n$ satisfy*

$$\boldsymbol{G} \succeq \boldsymbol{O}, \quad \boldsymbol{W} \succeq \boldsymbol{O}, \quad \boldsymbol{G}\boldsymbol{W} = \boldsymbol{O}$$

if and only if there exists a $\boldsymbol{Q} \in \mathbf{R}^{n \times n}$, with $\boldsymbol{Q}^\top \boldsymbol{Q} = \boldsymbol{I}$, such that

$$\begin{aligned}
&\boldsymbol{G} = \boldsymbol{Q}^\top \mathbf{Diag}(g_1, \dots, g_n) \boldsymbol{Q}, \\
&\boldsymbol{W} = \boldsymbol{Q}^\top \mathbf{Diag}(w_1, \dots, w_n) \boldsymbol{Q}, \\
&g_i \geq 0, \quad w_i \geq 0, \quad g_i w_i = 0 \quad (i = 1, \dots, n).
\end{aligned}$$

Proof. See Alizadeh *et al.* [2, Lemma 3]. □

We see that g_i and w_i introduced in Proposition 2.2 correspond to eigenvalues, or principal values in terminology of tensor analysis, of $\boldsymbol{G}$ and $\boldsymbol{W}$, respectively. The columns of $\boldsymbol{Q}$ coincide with the corresponding eigenvectors, or principal directions, of $\boldsymbol{G}$ and $\boldsymbol{W}$. Hence, Proposition 2.2 implies that $\boldsymbol{G}(\boldsymbol{Z})$ and $\boldsymbol{W}$ commute at the optimal solutions of the nonlinear SDP problem (7), i.e., they share a common system of eigenvectors. Moreover, the eigenvalues of $\boldsymbol{G}(\boldsymbol{Z})$ and $\boldsymbol{W}$ satisfy the complementarity conditions.

3 Minimization problem of total potential energy

Let $\mu \in \{2, 3\}$. Consider a μ-dimensional elastic body, which consists of isotropic material, and occupies a bounded and connected domain $\Omega \subset \mathbf{R}^\mu$ with a sufficiently smooth boundary $\partial\Omega$. The displacements vector field of the body is denoted by a mapping $\boldsymbol{u} : \Omega \mapsto \mathbf{R}^\mu$, which is also assumed to be smooth enough. The linear strain tensor $\boldsymbol{E}$ is defined by

$$\boldsymbol{E} = \frac{1}{2} \left[(\boldsymbol{u} \otimes \nabla) + (\boldsymbol{u} \otimes \nabla)^\top \right],$$

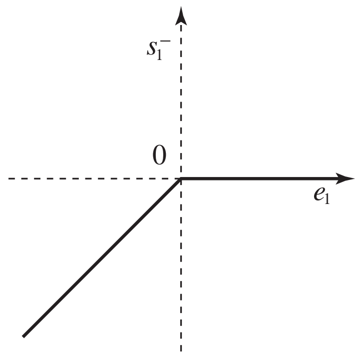

Figure 1: Constitutive law of no-tension material ($s_2^- = s_3^- = 0$).

which is a μ-dimensional symmetric second-order tensor. For simplicity, we often write

$$\mathcal{E} \cdot \boldsymbol{u} = \frac{1}{2} \left[(\boldsymbol{u} \otimes \nabla) + (\boldsymbol{u} \otimes \nabla)^\top \right], \tag{12}$$

where $\mathcal{E} : \mathbf{R}^\mu \mapsto \mathcal{S}^\mu$ can be regarded as the linear mapping introduced in (1).

Throughout this paper, by *no-tension material* we mean an elastic body which cannot transmit tension stresses, but otherwise behave as the linear elastic material. Hence, in general, the strain $\boldsymbol{E}$ is divided to the elastic components and the inelastic components referred to as cracks. We further assume that the inelastic strain components are reversible and non-dissipative, and that the stress components are path-independent. The no-tension material is widely used as a model of historical masonry structures, concrete structures, etc. [1, 11, 20]. In this paper, a structure consisting only of no-tension material is referred to as a *masonry structure*. Similarly, by *no-compression material* we mean an elastic body which cannot transmit compression stresses, but otherwise behave as the linear elastic material [9, 19]. The inelastic strain components are interpreted as wrinkling. *Membrane* in this paper means a two-dimensional structure which consists only of no-compression material. Sponge may be regarded as an example of three-dimensional structure consisting only of no-compression material.

Consider the linear material obeying Hooke's law such that the stress tensor $\boldsymbol{Q} \in \mathcal{S}^\mu$ for the strain $\boldsymbol{E} \in \mathcal{S}^\mu$ is given as

$$\boldsymbol{Q} = \mathsf{C} : \boldsymbol{E}, \tag{13}$$

where C denotes the constant forth-order elastic tensor. We assume that C is positive definite in the sense that $\boldsymbol{E} : \mathsf{C} : \boldsymbol{E} > 0$ for any $\mathcal{S}^\mu \ni \boldsymbol{E} \neq \boldsymbol{O}$. Then the strain energy function $\widetilde{w} : \mathcal{S}^\mu \mapsto \mathbf{R}$ of Hooke's material is obtained as

$$\widetilde{w}(\boldsymbol{E}) = \frac{1}{2} \boldsymbol{E} : \mathsf{C} : \boldsymbol{E}. \tag{14}$$

Let $\boldsymbol{S}^- \in \mathcal{S}^\mu$ denote the stress of no-tension material compatible to $\boldsymbol{E}$. It follows from the assumption of isotropy of material that $\boldsymbol{E}$ and $\boldsymbol{S}^-$ always commute, i.e., they always share a

Table 1: Definitions of strains and stresses.

	no-tension	Hooke (i)	Hooke (ii)
strain	$\boldsymbol{E}$	$\boldsymbol{E}$	$\boldsymbol{Z}$
stress	$\boldsymbol{S}^{-}$	$\boldsymbol{Q}$	$\boldsymbol{S}^{-}$
constitutive law	(15)–(17)	$\boldsymbol{Q} = \mathsf{C} : \boldsymbol{E}$	$\boldsymbol{S}^{-} = \mathsf{C} : \boldsymbol{Z}$

common system of eigenvectors. e_i and s_i^{-} $(i = 1, \dots, \mu)$, respectively, denote the principal strains and stresses. We introduce an auxiliary variable $\boldsymbol{Z} \in \mathcal{S}^{\mu}$ such that $(\boldsymbol{E} - \boldsymbol{Z})$ corresponds to the inelastic strain components due to crack opening. The principal values of $\boldsymbol{Z}$ are denoted by z_i $(i = 1, \dots, \mu)$. The constitutive law of no-tension material is given as

$$\boldsymbol{S}^{-} = \mathsf{C} : \boldsymbol{Z}, \tag{15}$$

$$\boldsymbol{E} \text{ and } (\boldsymbol{E} - \boldsymbol{Z}) \text{ commute}, \quad \begin{cases} e_i - z_i = 0, & \text{if } s_i^{-} < 0 \\ s_i^{-} = 0, & \text{if } e_i - z_i > 0 \end{cases} \tag{16}$$

$$s_i^{-} \leq 0, \quad e_i - z_i \geq 0 \quad (i = 1, \dots, \mu). \tag{17}$$

We give some remarks regarding the constitutive law (15)–(17). Recall that the no-tension material cannot transmit tension stresses. Hence, the principal stresses should be nonpositive anywhere, which is expressed as the first condition in (17). Fig.1 illustrates the relation between the principal stress s_1^{-} and the principal strain e_1 of no-tension material, in the case of $s_2^{-} = s_3^{-} = 0$. The second condition in (17) requires that the inelastic principal strains $(e_i - z_i)$ should be nonnegative, since they correspond to the amounts of opening crack. From the isotropy of material, we see that cracks should possibly open in the principal directions of strain, i.e., $(\boldsymbol{E} - \boldsymbol{Z})$ and $\boldsymbol{E}$ share a common system of eigenvectors. If infinitesimal tension stresses are applied, then the material immediately losses the stiffness in the corresponding principal directions as a consequence of smeared crack opening. On the other hand, if the principal stress s_i^{-} is negative, then no crack opens in the corresponding principal direction. These three conditions are guaranteed by (16). If there exists no crack, then the no-tension material obeys Hooke's law, which is represented by (15).

Let $\boldsymbol{S}^{-} = (S_{ij}^{-})$ and $\boldsymbol{E} = (E_{ij})$. $w^{-} : \mathcal{S}^{\mu} \mapsto \mathbf{R}$ denotes the strain energy function of no-tension material defined by

$$S_{ij}^{-} = \frac{\partial w^{-}}{\partial E_{ij}}, \quad w^{-}(\boldsymbol{O}) = 0, \tag{18}$$

or, equivalently,

$$w^{-}(\boldsymbol{E}) = \int \boldsymbol{S}^{-} : \mathrm{d}\boldsymbol{E}, \quad w^{-}(\boldsymbol{O}) = 0. \tag{19}$$

Notice again that $\boldsymbol{E}$ denotes the actual strain which is compatible to the displacement field $\boldsymbol{u}$. $\boldsymbol{Q}$ defined by (13) is regarded as the 'fictitious' stress compatible to $\boldsymbol{E}$, which is observed if the elastic body obeys Hooke's law without any crack. Alternatively, we also have the 'fictitious' strain $\boldsymbol{Z}$ of Hooke's material, which is compatible to $\boldsymbol{S}^-$ in the sense of (15). $(\boldsymbol{E}, \boldsymbol{S}^-)$ corresponds to the pair of strain and stress which is actually observed in the no-tension material. Table 1 summarizes the relation among $\boldsymbol{E}$, $\boldsymbol{Z}$, $\boldsymbol{S}^-$, and $\boldsymbol{Q}$. It should be emphasized that the sufficient condition (16) for absence of crack does not depend on $\boldsymbol{Q}$ defined by (13) but $\boldsymbol{S}^-$ defined by (15). For example, let $\mu = 2$, and let q_1 and q_2 denote the principal values of $\boldsymbol{Q}$. Suppose that $q_1 > 0$, $q_2 < 0$, $e_1 > 0$, and $e_2 > 0$, where Poisson's ratio is sufficiently large, and $|q_2|$ is sufficiently small compared with $|q_1|$. It follows from $e_1 > 0$ and $e_2 > 0$ that $\boldsymbol{S}^- = \boldsymbol{O}$, and hence $\boldsymbol{Z} = \boldsymbol{O}$ is obtained from (15), i.e., crack open both in the two principal directions. Consequently, this example illustrates that $q_2 < 0$ does not necessarily imply $z_2 - e_2 = 0$.

We assume small deformation as well as small strain. Let $\boldsymbol{t}$ denote the traction at boundary $\partial\Omega$ per unit length or area, depending on $\mu = 2$ or 3. Suppose that the boundary conditions $\boldsymbol{u} = \underline{\boldsymbol{u}}$ and $\boldsymbol{t} = \underline{\boldsymbol{t}}$ are given on $\Gamma_u \subset \partial\Omega$ and $\Gamma_t = \{\partial\Omega \setminus \Gamma_u\}$, respectively. By using (12) and (18), the minimization problem of total potential energy for masonry structures is formulated in variables $\boldsymbol{E}$ and $\boldsymbol{u}$ as

$$\left.\begin{aligned} (\Pi^-): \quad & \min \quad \int_\Omega (w^-(\boldsymbol{E}) - \boldsymbol{f}\cdot\boldsymbol{u})\,\mathrm{d}\Omega - \int_{\Gamma_t} \underline{\boldsymbol{t}}\cdot\boldsymbol{u}\mathrm{d}\Gamma \\ & \text{s.t.} \quad \boldsymbol{E} = \mathcal{E}\cdot\boldsymbol{u} \quad (\text{in } \Omega), \\ & \qquad\ \ \boldsymbol{u} - \underline{\boldsymbol{u}} = \boldsymbol{0} \quad (\text{on } \Gamma_u). \end{aligned}\right\} \tag{20}$$

Remark 3.1. Recall that, for the no-compression material, we assume that the principal stresses are nonnegative, i.e., the stress $\boldsymbol{S}^+$ should be positive semidefinite. Hence, compared with the case of no-tension material given by (15)–(17), the constitutive law of no-compression material is given as

$$\boldsymbol{S}^+ = \mathbf{C} : \boldsymbol{Z}, \tag{21}$$

$$\boldsymbol{E} \text{ and } (\boldsymbol{Z} - \boldsymbol{E}) \text{ commute}, \quad \begin{cases} z_i - e_i = 0, & \text{if } s_i^+ > 0 \\ s_i^+ = 0, & \text{if } z_i - e_i > 0 \end{cases} \tag{22}$$

$$s^+ \geq 0, \quad z_i - e_i \geq 0 \quad (i = 1, \dots, \mu). \tag{23}$$

Here, $(\boldsymbol{Z} - \boldsymbol{E})$ describes the amount of wrinkle. By using (21)–(23), the strain energy w^+ is defined in a similar manner to (18). Consequently, the minimization problem of total potential energy for membranes can be obtained by replacing w^- in Problem (20) with w^+. □

Throughout this paper, $(\ )^-$ and $(\ )^+$ denote the quantities or functions for no-tension and no-compression materials, respectively.

4 Infinite-dimensional SDP formulation

The constitutive law introduced in Section 3 guarantees that the stress of no-tension material is path-independent, and masonry structures have no energy dissipation. Hence, the principle of minimum total potential energy can be applied to a masonry structure, and an equilibrium configuration is obtained as a solution of Problem (20). From (15)–(18), however, we see that the objective function of Problem (20) depends on both the principal values and principal directions of $\boldsymbol{E}$. Hence, it is not recommended to solve Problem (20) directly. This motivates us to reformulate Problem (20) as the (infinite-dimensional version of) SDP problem.

The following lemma shows that the constitutive law of no-tension material is expressed by using the complementarity condition in terms of positive semidefinite matrices:

Lemma 4.1. *$\boldsymbol{E}$, $\boldsymbol{S}^-$, and $\boldsymbol{Z}$ satisfy the constitutive law* (15)–(17) *of no-tension material if and only if they satisfy* (15) *and*

$$\boldsymbol{E} - \boldsymbol{Z} \succeq \boldsymbol{O}, \quad -\boldsymbol{S}^- \succeq \boldsymbol{O}, \quad \boldsymbol{S}^- : (\boldsymbol{E} - \boldsymbol{Z}) = 0. \tag{24}$$

Proof. It suffices to show under (15) that the condition (24) is equivalent to (16) and (17). Let λ_i $(i = 1, \dots, \mu)$ denote the principal values of the tensor $(\boldsymbol{E} - \boldsymbol{Z})$. It follows from Proposition 2.2 that (24) holds if and only if $\boldsymbol{S}^-$ and $(\boldsymbol{E} - \boldsymbol{Z})$ satisfy

$$\boldsymbol{S}^- \text{ and } (\boldsymbol{E} - \boldsymbol{Z}) \text{ commute}, \tag{25}$$

$$\lambda_i \geq 0, \quad -s_i^- \geq 0, \quad s_i^- \lambda_i = 0 \quad (i = 1, \dots, \mu). \tag{26}$$

The assumption of isotropy of no-tension material and (15) imply that $\boldsymbol{S}^-$ and $\boldsymbol{Z}$ commute. Hence, (25) implies $\boldsymbol{S}^-$ and $\boldsymbol{E}$ also commute, i.e., $\boldsymbol{S}^-$, $\boldsymbol{E}$ and $\boldsymbol{Z}$ commute, from which it follows that (25) and (26) hold if and only if (25) and

$$e_i - z_i \geq 0, \quad -s_i^- \geq 0, \quad s_i^- (e_i - z_i) = 0 \quad (i = 1, \dots, \mu) \tag{27}$$

are satisfied. Consequently, (24) is equivalent to (25) and (27). Then we can easily see that (16) and (17) are equivalent to (25) and (27). □

The system of (15) and (24) is often referred to as the *semidefinite linear complementarity problem* (*SDLCP*) [18], and Lemma 4.1 implies that the constitutive law of no-tension material can be expressed as the SDLCP. Recently, one of the authors formulated the three-dimensional frictional contact problem as the second-order cone linear complementarity problem [14], which is a particular case of the SDLCP. From the mechanical point of view, the complementarity condition $\boldsymbol{S}^- : (\boldsymbol{E} - \boldsymbol{Z}) = 0$ in (24) implies that $(\boldsymbol{E} - \boldsymbol{Z})$ does not contribute to the strain energy, i.e., $(\boldsymbol{E} - \boldsymbol{Z})$ coincides with the amount of smeared crack.

The following lemma gives the relation between the strain energy w^- of no-tension material and $\widetilde{w}$ of Hooke's material:

Lemma 4.2. *w^- and $\widetilde{w}$ defined by* (14)–(18) *satisfy*

$$w^-(\boldsymbol{E}) = \min_{\boldsymbol{Z}\in\mathcal{S}^\mu} \{\widetilde{w}(\boldsymbol{Z}) | \, \boldsymbol{Z} \preceq \boldsymbol{E}\}. \tag{28}$$

Proof. Observe that the right hand side of (28) is regarded as the nonlinear SDP problem in variable $\boldsymbol{Z} \in \mathcal{S}^\mu$. Indeed, this problem is embedded into Problem (7) by putting

$$f(\boldsymbol{Z}) := \frac{1}{2}\boldsymbol{Z} : \mathsf{C} : \boldsymbol{Z}, \quad \boldsymbol{G}(\boldsymbol{Z}) := -\boldsymbol{Z} + \boldsymbol{E}.$$

It follows from Proposition 2.1 and the convexity of f and $\boldsymbol{G}$ that $\boldsymbol{Z}$ is an optimal solution of this problem if and only if there exists a $\boldsymbol{W} \in \mathcal{S}^n$ satisfying the following KKT conditions:

$$\mathsf{C} : \boldsymbol{Z} + \boldsymbol{W} = \boldsymbol{O}, \tag{29}$$

$$-\boldsymbol{Z} + \boldsymbol{E} \succeq \boldsymbol{O}, \quad \boldsymbol{W} \succeq \boldsymbol{O}, \quad \boldsymbol{W} : (-\boldsymbol{Z} + \boldsymbol{E}) = 0. \tag{30}$$

By putting $\boldsymbol{W} := -\boldsymbol{S}^-$, we see that the conditions (29) and (30) are equivalent to

$$\boldsymbol{S}^- = \mathsf{C} : \boldsymbol{Z}, \tag{31}$$

$$\boldsymbol{E} - \boldsymbol{Z} \succeq \boldsymbol{O}, \quad -\boldsymbol{S}^- \succeq \boldsymbol{O}, \quad \boldsymbol{S}^- : (\boldsymbol{E} - \boldsymbol{Z}) = 0, \tag{32}$$

from which and Lemma 4.1 it follows that an optimal solution $\boldsymbol{Z}$ and the corresponding Lagrange multiplier $\boldsymbol{S}^-$ of the problem on the right hand side of (28) satisfy (15)–(17), i.e., if $\boldsymbol{Z}$ is an optimal solution, then (31) is satisfied with the stress $\boldsymbol{S}^-$ of no-tension material compatible to the strain $\boldsymbol{E}$. Recall that w^- is defined by (19). By using (31) and the equality in (32), we obtain

$$\boldsymbol{S}^- : \mathrm{d}\boldsymbol{E} = \boldsymbol{S}^- : \mathrm{d}\boldsymbol{Z} = \boldsymbol{Z} : \mathsf{C} : \mathrm{d}\boldsymbol{Z}.$$

Hence, from (19), the implication

$$w^-(\boldsymbol{E}) = \int \boldsymbol{S}^- : \mathrm{d}\boldsymbol{E} = \int \boldsymbol{Z} : \mathsf{C} : \mathrm{d}\boldsymbol{Z} = \frac{1}{2}\boldsymbol{Z} : \boldsymbol{C} : \boldsymbol{Z} = \widetilde{w}(\boldsymbol{Z})$$

holds if (31) and (32) are satisfied. We have seen that the latter condition is equivalent to the fact that $\boldsymbol{Z}$ is an optimal solution of the problem on the right hand side of (28), which completes the proof. □

Recall that an equilibrium configuration of the masonry structure is characterized as an optimal solution of Problem (20). As our main result in this section, by using Lemma 4.2, we reformulate Problem (20) into the (infinite-dimensional) SDP problem as follows:

Lemma 4.3. $(\boldsymbol{E}^*, \boldsymbol{u}^*)$ *is an optimal solution of Problem* (20) *if and only if* $(\boldsymbol{Z}^*, \boldsymbol{u}^*)$ *is an optimal solution of the following problem in variables* $\boldsymbol{Z}$ *and* $\boldsymbol{u}$*:*

$$\left.\begin{aligned} (\mathrm{P}^-): \quad \min \quad & \int_\Omega (\widetilde{w}(\boldsymbol{Z}) - \boldsymbol{f}\cdot\boldsymbol{u})\,\mathrm{d}\Omega - \int_{\Gamma_t} \underline{\boldsymbol{t}}\cdot\boldsymbol{u}\mathrm{d}\Gamma \\ \mathrm{s.t.} \quad & \boldsymbol{Z} \preceq \mathcal{E}\cdot\boldsymbol{u} \quad (\text{in } \Omega), \\ & \boldsymbol{u} - \underline{\boldsymbol{u}} = \boldsymbol{0} \quad (\text{on } \Gamma_u), \end{aligned}\right\} \tag{33}$$

where

$$\boldsymbol{E}^* = \mathcal{E} \cdot \boldsymbol{u}^*, \tag{34}$$

$$\boldsymbol{Z}^* = \mathsf{C}^{-1} : \boldsymbol{S}^{-*}, \quad S_{ij}^{-*} = \left.\frac{\partial w^-(\boldsymbol{E})}{\partial E_{ij}}\right|_{\boldsymbol{E}=\boldsymbol{E}^*}. \tag{35}$$

Proof. By using Lemma 4.2, Problem (20) is equivalent to

$$\left.\begin{array}{ll} \min & \displaystyle\int_\Omega \left(\min_{\boldsymbol{Z}\in\mathcal{S}^\mu} \{ \widetilde{w}(\boldsymbol{Z}) \,|\, \boldsymbol{Z} \preceq \boldsymbol{E} \} - \boldsymbol{f}\cdot\boldsymbol{u} \right) \mathrm{d}\Omega - \int_{\Gamma_t} \underline{\boldsymbol{t}}\cdot\boldsymbol{u}\mathrm{d}\Gamma \\ \mathrm{s.t.} & \boldsymbol{E} = \mathcal{E}\cdot\boldsymbol{u} \quad (\text{in } \Omega), \\ & \boldsymbol{u} - \underline{\boldsymbol{u}} = \boldsymbol{0} \quad (\text{on } \Gamma_u). \end{array}\right\} \tag{36}$$

Observe that, in Problem (36), only $\boldsymbol{Z} \preceq \boldsymbol{E}$ in the inner problem is the constraint on $\boldsymbol{Z}$. Hence, Problem (36) is equivalent to the following problem in variables $\boldsymbol{Z}$, $\boldsymbol{E}$, and $\boldsymbol{u}$:

$$\left.\begin{array}{ll} \min & \displaystyle\int_\Omega (\widetilde{w}(\boldsymbol{Z}) - \boldsymbol{f}\cdot\boldsymbol{u})\, \mathrm{d}\Omega - \int_{\Gamma_t} \underline{\boldsymbol{t}}\cdot\boldsymbol{u}\mathrm{d}\Gamma \\ \mathrm{s.t.} & \boldsymbol{Z} \preceq \boldsymbol{E}, \quad \boldsymbol{E} = \mathcal{E}\cdot\boldsymbol{u} \quad (\text{in } \Omega), \\ & \boldsymbol{u} - \underline{\boldsymbol{u}} = \boldsymbol{0} \quad (\text{on } \Gamma_u). \end{array}\right\} \tag{37}$$

It follows from the proof of Lemma 4.2 that (31) and (32) hold at an optimal solution of Problem (36). Since Problem (36) is equivalent to Problem (37), and by using Lemma 4.1, we see that (35) is satisfied if $(\boldsymbol{Z}^*, \boldsymbol{E}^*, \boldsymbol{u}^*)$ is an optimal solution of Problem (37). Moreover, (34) holds at an optimal solution of Problem (37). Consequently, $(\boldsymbol{E}^*, \boldsymbol{u}^*)$ defined by (34) is an optimal solution of Problem (20) if and only if $(\boldsymbol{Z}^*, \boldsymbol{E}^*, \boldsymbol{u}^*)$ defined by (35) is an optimal solution of Problem (37). □

Lemma 4.3 implies that the equilibrium configuration $\boldsymbol{u}^*$ of the masonry structure is obtained by solving Problem (33) instead of Problem (20). Problem (33) is reduced to the following problem in variables $\boldsymbol{Z}$, $\boldsymbol{u}$ and τ:

$$\left.\begin{array}{ll} \min & \displaystyle\int_\Omega (\tau - \boldsymbol{f}\cdot\boldsymbol{u})\, \mathrm{d}\Omega - \int_{\Gamma_t} \underline{\boldsymbol{t}}\cdot\boldsymbol{u}\mathrm{d}\Gamma \\ \mathrm{s.t.} & \tau \geq \dfrac{1}{2}\boldsymbol{Z} : \mathsf{C} : \boldsymbol{Z}, \quad \mathcal{E}\cdot\boldsymbol{u} - \boldsymbol{Z} \succeq \boldsymbol{O} \quad (\text{in } \Omega), \\ & \boldsymbol{u} = \underline{\boldsymbol{u}} \quad (\text{on } \Gamma_u). \end{array}\right\} \tag{38}$$

In Problem (38), it is known that the convex quadratic inequality

$$\tau \geq \frac{1}{2}\boldsymbol{Z} : \mathsf{C} : \boldsymbol{Z} \tag{39}$$

can be written as the linear matrix inequality in terms of τ and $\boldsymbol{Z}$ [4, Section 4.2]. However, in Section 5, we transform (39) into a second-order cone [4, Section 3.3], which is also representable as a linear matrix inequality. It follows from the definition (12) of $\mathcal{E}$ that the constraint

$$\mathcal{E}\cdot\boldsymbol{u} - \boldsymbol{Z} \succeq \boldsymbol{O}$$

is also the linear matrix inequality. Consequently, all the constraints of Problem (38) can be represented as the linear matrix inequalities. Moreover, Problem (38) has the linear objective function. Hence, Problem (38) is regarded as an SDP problem with the infinitely many variables. This is important because the finite-dimensional SDP is the convex optimization problem which can be solved efficiently by using the primal-dual interior-point method [18, 29]. Moreover, the formulations of Problems (33) and (38) are independent of the existence and directions of cracks. Hence, we can obtain the equilibrium configuration as an optimal solution of Problem (33) or (38) without any assumption on cracks and/or stress states. We show in Section 5 that Problem (33) is reduced to the SDP problem with finite number of variables by using the conventional finite-element discretization.

Remark 4.4. The strain energy function w^+ of no-compression material was defined in Remark 3.1. In a similar manner to Lemma 4.2, we can show that w^+ satisfies

$$w^+(\boldsymbol{E}) = \min_{\boldsymbol{Z} \in \mathcal{S}^\mu} \{ \widetilde{w}(\boldsymbol{Z}) \big| \boldsymbol{Z} \succeq \boldsymbol{E} \}.$$

Hence, in a manner similar to Lemma 4.3, the minimization problem of total potential energy for membrane can be reformulated as

$$\left.\begin{array}{lll} (\mathrm{P}^+): & \min & \displaystyle\int_\Omega (\widetilde{w}(\boldsymbol{Z}) - \boldsymbol{f} \cdot \boldsymbol{u}) \, \mathrm{d}\Omega - \int_{\Gamma_t} \underline{\boldsymbol{t}} \cdot \boldsymbol{u} \mathrm{d}\Gamma \\ & \mathrm{s.t.} & \boldsymbol{Z} \succeq \mathcal{E} \cdot \boldsymbol{u} \quad (\text{in } \Omega), \\ & & \boldsymbol{u} - \underline{\boldsymbol{u}} = \boldsymbol{0} \quad (\text{on } \Gamma_u). \end{array}\right\} \tag{40}$$

Moreover, by introducing an auxiliary variable τ in a manner similar to Problem (38), we see that Problem (40) is equivalent to

$$\left.\begin{array}{ll} \min & \displaystyle\int_\Omega (\tau - \boldsymbol{f} \cdot \boldsymbol{u}) \, \mathrm{d}\Omega - \int_{\Gamma_t} \underline{\boldsymbol{t}} \cdot \boldsymbol{u} \mathrm{d}\Gamma \\ \mathrm{s.t.} & \tau \geq \dfrac{1}{2} \boldsymbol{Z} : \mathbf{C} : \boldsymbol{Z}, \quad \boldsymbol{Z} - \mathcal{E} \cdot \boldsymbol{u} \succeq \boldsymbol{O} \quad (\text{in } \Omega), \\ & \boldsymbol{u} - \underline{\boldsymbol{u}} = \boldsymbol{0} \quad (\text{on } \Gamma_u), \end{array}\right\} \tag{41}$$

which is also an infinite-dimensional SDP problem. □

5 Finite element discretization of Problem (33)

In Section 4, we have established the convex (infinite-dimensional) variational problems for masonry structures and membranes. Since Problems (33) and (40) include an auxiliary variable $\boldsymbol{Z}$, these formulations are not suitable for constructing the conventional tangential stiffness. In this section, we show that Problems (33) and (40) are discretized into the finite-dimensional SDP problems, without constructing the tangent stiffness matrix. The resulting SDP problems are solved by using the primal-dual interior-point method [29]. Thus, the discretization scheme in this section is essentially required for our solution technique.

Suppose that Ω is divided into $n^{\rm m}$ isoparametric finite elements, each of which occupies $\Omega^{l} \subset \mathbf{R}^{\mu}$ $(l = 1, \dots, n^{\rm m})$. Let $\boldsymbol{a}^{l} \in \mathbf{R}^{n_{\rm e}^{\rm d}}$ denote the displacements in the global coordinates $\boldsymbol{x} = (x_j) \in \mathbf{R}^{\mu}$ at the nodes belonging to the l-th element, where $n_{\rm e}^{\rm d}$ denotes the number of degrees of freedom of each element. $\boldsymbol{r} = (r_j) \in \mathbf{R}^{\mu}$ denotes the reference frame of the natural coordinates of the isoparametric element [30]. The Jacobian matrix $\boldsymbol{J}$ is defined by $\mathrm{d}\boldsymbol{x} = \boldsymbol{J}\mathrm{d}\boldsymbol{r}$.

Assume that the vector field of displacements $\boldsymbol{u} \in \mathbf{R}^{\mu}$ in Ω^{l} in the global coordinates is approximated as

$$\boldsymbol{u} \simeq \boldsymbol{N}(\boldsymbol{r}) \cdot \boldsymbol{a}^{l} \quad (\text{in } \Omega^{l}), \tag{42}$$

where $\boldsymbol{N}(\boldsymbol{r}) \in \mathbf{R}^{\mu \times n_{\rm e}^{\rm d}}$ is a matrix of shape function given in the element natural coordinate $\boldsymbol{r}$ [30]. Recall that the action of linear mapping $\mathcal{E}$ on $\boldsymbol{u}$ was defined by (12), which includes the differential operations with respect to the global coordinate. Letting $\mathcal{B} = \mathcal{E} \cdot \boldsymbol{N}$, and by using (42), we see

$$\mathcal{E} \cdot \boldsymbol{u} = \mathcal{B}(\boldsymbol{r}) \cdot \boldsymbol{a}^{l}, \tag{43}$$

where $\mathcal{B} : \mathbf{R}^{n_{\rm e}^{\rm d}} \mapsto \mathcal{S}^{\mu}$. Let $\boldsymbol{w} \in \mathbf{R}^{n^{\rm d}}$ denote the vector of nodal displacements of the discretized structure, where $n^{\rm d}$ is the number of degrees of freedom after removing the constrained degrees of freedom by supports. $n_{\rm f}^{\rm d}$ and $n_{\rm p}^{\rm d}$, respectively, denote the numbers of unconstrained degrees of freedom and degrees of freedom of prescribed displacements, where $n_{\rm f}^{\rm d} + n_{\rm p}^{\rm d} = n^{\rm d}$. The relation between $\boldsymbol{w}$ and $\boldsymbol{a}^{l}$ can be written as

$$\boldsymbol{a}^{l} = \boldsymbol{T}_{\rm f}^{l} \cdot \boldsymbol{w}, \tag{44}$$

where $\boldsymbol{T}_{\rm f}^{l} \in \mathbf{R}^{n_{\rm e}^{\rm d} \times n^{\rm d}}$ is a constant assignment matrix for each $l = 1, \dots, n^{\rm m}$. Letting $\underline{\widehat{\boldsymbol{w}}} \in \mathbf{R}^{n_{\rm p}^{\rm d}}$ denote the vector of prescribed displacements, the boundary condition $\boldsymbol{u} - \underline{\boldsymbol{u}} = \boldsymbol{0}$ on Γ_u in Problem (20) is discretized as

$$\boldsymbol{T}_{\rm p} \cdot \boldsymbol{w} - \underline{\widehat{\boldsymbol{w}}} = \boldsymbol{0}, \tag{45}$$

where $\boldsymbol{T}_{\rm p} \in \mathbf{R}^{n_{\rm p}^{\rm d} \times n^{\rm d}}$ is also a constant matrix.

Observe that the first term of the objective function of Problem (33) is reduced to

$$\int_{\Omega} \widetilde{w}(\boldsymbol{Z}) \mathrm{d}\Omega = \sum_{l=1}^{n^{\rm m}} \int_{\Omega^{l}} \widetilde{w}(\boldsymbol{Z}) \mathrm{d}\Omega. \tag{46}$$

The integration on the right-hand side of (46) is calculated numerically by using the Gauss quadrature. Consider $n^{\rm g}$ sampling points of the Gauss formulas for each element Ω^{l}. Then the integration in (46) is approximated as

$$\int_{\Omega^{l}} \widetilde{w}(\boldsymbol{Z}) \mathrm{d}\Omega \simeq \sum_{i=1}^{n^{\rm g}} \rho_i \widetilde{w}(\boldsymbol{r}_i) \det \boldsymbol{J}(\boldsymbol{r}_i), \tag{47}$$

where $\boldsymbol{r}_i$ and ρ_i ($i = 1, \dots, n^{\rm g}$), respectively, denote the coordinates of sampling points and weights of Gauss quadrature. For simplicity, we define $\widehat{\rho}_i$ by

$$\widehat{\rho}_i = \rho_i \det \boldsymbol{J}(\boldsymbol{r}_i) \quad (i = 1, \dots, n^{\rm g}).$$

In accordance with (47), we evaluate $\boldsymbol{Z}$ in Problem (33) at the sampling points $\boldsymbol{r}_i$ for the Gauss integration. Letting

$$\boldsymbol{Z}_i^l := \boldsymbol{Z}(\boldsymbol{r}_i) \quad (\text{in } \Omega^l),$$

for each $i = 1, \dots, n^{\rm g}$, we have

$$\widetilde{w}(\boldsymbol{r}_i) = \frac{1}{2} \boldsymbol{Z}_i^l : \mathbf{C} : \boldsymbol{Z}_i^l \tag{48}$$

from (14). Similarly, letting $\mathcal{B}_i := \mathcal{B}(\boldsymbol{r}_i)$, and by using (43), we have

$$\mathcal{E} \cdot \boldsymbol{u} = \mathcal{B}_i \cdot \boldsymbol{T}_{\rm f}^l \cdot \boldsymbol{w} \quad (\text{in } \Omega^l) \tag{49}$$

at each sampling points. Let $\underline{\boldsymbol{f}} \in \mathbf{R}^{n_{\rm f}^{\rm d}}$ denote the discretized external force vector, which is applied to the unconstrained degrees of freedom. $\widehat{\underline{\boldsymbol{f}}} \in \mathbf{R}^{n^{\rm d}}$ denotes the vector consisting of all elements of $\underline{\boldsymbol{f}}$ and 0 for constrained degrees. By using (45)–(49), Problem (33) is discretized into the following finite-dimensional problem:

$$\left. \begin{array}{lll} (\mathrm{P}_{\rm FEM}^{-}) : & \min & \displaystyle\sum_{l=1}^{n^{\rm m}} \sum_{i=1}^{n^{\rm g}} \frac{\widehat{\rho}_i}{2} \boldsymbol{Z}_i^l : \mathbf{C} : \boldsymbol{Z}_i^l - \widehat{\underline{\boldsymbol{f}}} \cdot \boldsymbol{w} \\ & \text{s.t.} & -\boldsymbol{Z}_i^l + \mathcal{B}_i \cdot \boldsymbol{T}_{\rm f}^l \cdot \boldsymbol{w} \succeq \boldsymbol{O} \quad (i = 1, \dots, n^{\rm g};\ l = 1, \dots, n^{\rm m}), \\ & & \boldsymbol{T}_{\rm p} \cdot \boldsymbol{w} - \widehat{\underline{\boldsymbol{w}}} = \boldsymbol{0}, \end{array} \right\} \tag{50}$$

where independent variables are $\boldsymbol{w} \in \mathbf{R}^{n^{\rm d}}$ and $\boldsymbol{Z}_i^l \in \mathcal{S}^{\mu}$ ($i = 1, \dots, n^{\rm g};\ l = 1, \dots, n^{\rm m}$).

The remainder of this section is devoted to showing that Problem (50) coincides with the (finite-dimensional) SDP problem, which enables us to utilize the existing well-developed softwares based on the primal-dual interior-point method for SDP.

Let $\|\boldsymbol{q}\|$ denote the standard Euclidean norm of $\boldsymbol{q} \in \mathbf{R}^n$ defined by $\|\boldsymbol{q}\| = (\boldsymbol{q}^\top \boldsymbol{q})^{1/2}$. $\mathbf{R}_+^n \subset \mathbf{R}^n$ and $\mathbf{L}_+^n \subset \mathbf{R}^n$ denote the non-negative orthant and the *second-order cone* [4], respectively, defined by

$$\mathbf{R}_+^n = \{\boldsymbol{p} = (p_1, \dots, p_n) \in \mathbf{R}^n | p_i \geq 0 \ (i = 1, \dots, n)\},$$
$$\mathbf{L}_+^n = \{\boldsymbol{p} = (p_0, \boldsymbol{p}_1) \in \mathbf{R} \times \mathbf{R}^{n-1} | p_0 \geq \|\boldsymbol{p}_1\|\}.$$

$\mathcal{S}_+^n \subset \mathcal{S}^n$ is defined by

$$\mathcal{S}_+^n = \{\boldsymbol{P} \in \mathcal{S}^n | \mathcal{S}^n \succeq \boldsymbol{O}\}.$$

In order to solve Problem (50), we use the primal-dual interior-point method for SDP, which finds an optimal solution of the SDP problem. Some of these softwares, e.g., SeDuMi [27], are designed to solve the (dual) SDP problems in the following form:

$$\left.\begin{array}{ll} \max & \boldsymbol{b}^\top \boldsymbol{y} \\ \text{s.t.} & \boldsymbol{c} - \boldsymbol{A}^\top \boldsymbol{y} \in \mathcal{K}, \end{array}\right\} \tag{51}$$

where

$$\mathcal{K} = \mathbf{R}_+^{n^{\mathrm{R}}} \times \mathbf{L}_+^{n_1^{\mathrm{L}}} \times \cdots \times \mathbf{L}_+^{n_p^{\mathrm{L}}} \times \mathcal{S}_+^{n_1^{\mathrm{S}}} \times \cdots \times \mathcal{S}_+^{n_q^{\mathrm{S}}}.$$

As known well, SDP includes LP and SOCP as particular cases [29]. Indeed, by taking $\mathcal{K} = \mathbf{R}_+^{n^{\mathrm{R}}}$ and $\mathcal{K} = \mathbf{L}_+^{n_1^{\mathrm{L}}} \times \cdots \times \mathbf{L}_+^{n_p^{\mathrm{L}}}$, Problem (51) is reduced to the LP and SOCP problems, respectively. We transforms Problem (50) into the form of Problem (51).

By introducing the auxiliary variables τ_i^l, Problem (50) is equivalent to the following problem formulated in variables $\boldsymbol{Z}_i^l$, $\boldsymbol{w}$, and τ_i^l:

$$\left.\begin{array}{ll} \min & \displaystyle\sum_{l=1}^{n^{\mathrm{m}}} \sum_{i=1}^{n^{\mathrm{g}}} \tau_i^l - \underline{\widehat{\boldsymbol{f}}} \cdot \boldsymbol{w} \\ \text{s.t.} & \tau_i^l \geq \dfrac{\widehat{\rho}_i}{2} \boldsymbol{Z}_i^l : \mathsf{C} : \boldsymbol{Z}_i^l, \quad -\boldsymbol{Z}_i^l + \mathcal{B}_i \cdot \boldsymbol{T}_{\mathrm{f}}^l \cdot \boldsymbol{w} \succeq \boldsymbol{O} \\ & \qquad (i = 1, \dots, n^{\mathrm{g}};\ l = 1, \dots, n^{\mathrm{m}}), \\ & \boldsymbol{T}_{\mathrm{p}} \cdot \boldsymbol{w} - \underline{\widehat{\boldsymbol{w}}} = \mathbf{0}. \end{array}\right\} \tag{52}$$

Recall that the operator **evec** has been introduced in (3), which expresses the transformation from a strain tensor into a strain vector. It follows from the positive definiteness of C that there exists a positive definite matrix $\widehat{\boldsymbol{C}} \in \mathcal{S}^{\widehat{\mu}}$ satisfying

$$\boldsymbol{Z} : \mathsf{C} : \boldsymbol{Z} = \mathbf{evec}(\boldsymbol{Z})^\top \widehat{\boldsymbol{C}}\, \mathbf{evec}(\boldsymbol{Z}),$$

where

$$\widehat{\mu} = \mu(\mu + 1)/2.$$

We introduce new variables $\boldsymbol{\zeta}_i^l \in \mathbf{R}^{\widehat{\mu}}$ $(i = 1, \dots, n^{\mathrm{g}};\ l = 1, \dots, n^{\mathrm{m}})$ by

$$\boldsymbol{\zeta}_i^l = \mathbf{evec}(\boldsymbol{Z}_i^l),$$

which is alternatively written as

$$\boldsymbol{Z}_i^l = \mathbf{Mat}(\boldsymbol{\zeta}_i^l).$$

Since $\widehat{\boldsymbol{C}}$ is nonsingular, there exists a $\boldsymbol{G} \in \mathbf{R}^{\widehat{\mu} \times \widehat{\mu}}$ satisfying $\widehat{\boldsymbol{C}} = \boldsymbol{G}^\top \boldsymbol{G}$. For example, we can choose $\boldsymbol{G}$ as the Cholesky factor of $\widehat{\boldsymbol{C}}$. Then the convex quadratic inequality

$$\tau_i^l \geq \frac{\widehat{\rho}_i}{2} \boldsymbol{\zeta}_i^{l\top} \widehat{\boldsymbol{C}} \boldsymbol{\zeta}_i^l$$

can be expressed via a second-order cone as [see 4, § 3.3.1]

$$\frac{\tau_i^l}{2\widehat{\rho}_i} + 1 \geq \left\| \begin{pmatrix} \dfrac{\tau_i^l}{2\widehat{\rho}_i} - 1 \\ \boldsymbol{G}\boldsymbol{\zeta}_i^l \end{pmatrix} \right\|.$$

Hence, Problem (52) is reduced to

$$\left.\begin{array}{ll} \min & \displaystyle\sum_{l=1}^{n^{\mathrm{m}}} \sum_{i=1}^{n^{\mathrm{g}}} \tau_i^l - \underline{\widehat{\boldsymbol{f}}} \cdot \boldsymbol{w} \\ \mathrm{s.t.} & \boldsymbol{T}_{\mathrm{p}} \cdot \boldsymbol{w} - \underline{\widehat{\boldsymbol{w}}} \in \mathbf{R}_+^{n_{\mathrm{p}}^{\mathrm{d}}}, \quad -\boldsymbol{T}_{\mathrm{p}} \cdot \boldsymbol{w} + \underline{\widehat{\boldsymbol{w}}} \in \mathbf{R}_+^{n_{\mathrm{p}}^{\mathrm{d}}}, \\ & \begin{pmatrix} \dfrac{\tau_i^l}{2\widehat{\rho}_i} + 1 \\ \dfrac{\tau_i^l}{2\widehat{\rho}_i} - 1 \\ \boldsymbol{G} \cdot \boldsymbol{\zeta}_i^l \end{pmatrix} \in \mathbf{L}_+^{\widehat{\mu}+2} \quad (i = 1, \dots, n^{\mathrm{g}};\ l = 1, \dots, n^{\mathrm{m}}), \\ & -\mathbf{Mat}(\boldsymbol{\zeta}_i^l) + \mathcal{B}_i \cdot \boldsymbol{T}_{\mathrm{f}}^l \cdot \boldsymbol{w} \in \mathcal{S}_+^{\mu} \quad (i = 1, \dots, n^{\mathrm{g}};\ l = 1, \dots, n^{\mathrm{m}}), \end{array}\right\} \quad (53)$$

where the independent variables are $(\boldsymbol{\zeta}, \boldsymbol{w}, \boldsymbol{\tau}) \in \mathbf{R}^{\widehat{\mu} n^{\mathrm{g}} n^{\mathrm{m}}} \times \mathbf{R}^{n^{\mathrm{d}}} \times \mathbf{R}^{n^{\mathrm{g}} n^{\mathrm{m}}}$ with $\boldsymbol{\zeta} = (\boldsymbol{\zeta}_1^1, \dots, \boldsymbol{\zeta}_{n^{\mathrm{m}}}^{n^{\mathrm{g}}})$ and $\boldsymbol{\tau} = (\tau_1^1, \dots, \tau_{n^{\mathrm{m}}}^{n^{\mathrm{g}}})$. Recall that the constraint with the **Mat** operator in the form of (4) is the linear matrix inequality, which appears in the dual standard form of SDP problem (6). Thus, we see that Problem (53) is embedded into Problem (51) with

$$\mathcal{K} = \mathbf{R}_+^{2n_{\mathrm{p}}^{\mathrm{d}}} \times (\mathbf{L}_+^{\widehat{\mu}+2} \times \mathcal{S}_+^{\mu})^{n^{\mathrm{g}} n^{\mathrm{m}}}.$$

It should be emphasized that Problem (53) is an SDP problem which can be solved efficiently by using the primal-dual interior-point method [29], and the number of arithmetic operations is bounded by a polynomial of μ, $n_{\mathrm{p}}^{\mathrm{d}}$, n^{g}, and n^{m}. Since the constitutive law (15)–(17) of no-tension material depends on the stress states, the conventional method based on the tangent stiffness requires assumptions of stress states, especially the existence and directions of cracks. On the other hand, Problem (53) can be solved without any assumption, which is regarded as the major advantage of our method.

Remark 5.1. In a similar manner to Problem (50), the finite-element discretization of Problem (40) for membrane is obtained as

$$\left.\begin{array}{lll} (\mathrm{P}_{\mathrm{FEM}}^{+}): & \min & \displaystyle\sum_{l=1}^{n^{\mathrm{m}}} \sum_{i=1}^{n^{\mathrm{g}}} \frac{\widehat{\rho}_i}{2} \boldsymbol{Z}_i^l : \mathbf{C} : \boldsymbol{Z}_i^l - \underline{\widehat{\boldsymbol{f}}} \cdot \boldsymbol{w} \\ & \mathrm{s.t.} & \boldsymbol{Z}_i^l - \mathcal{B}_i \cdot \boldsymbol{T}_{\mathrm{f}}^l \cdot \boldsymbol{w} \succeq \boldsymbol{O} \quad (i = 1, \dots, n^{\mathrm{g}};\ l = 1, \dots, n^{\mathrm{m}}), \\ & & \boldsymbol{T}_{\mathrm{p}} \cdot \boldsymbol{w} - \underline{\widehat{\boldsymbol{w}}} = \mathbf{0}. \end{array}\right\} \quad (54)$$

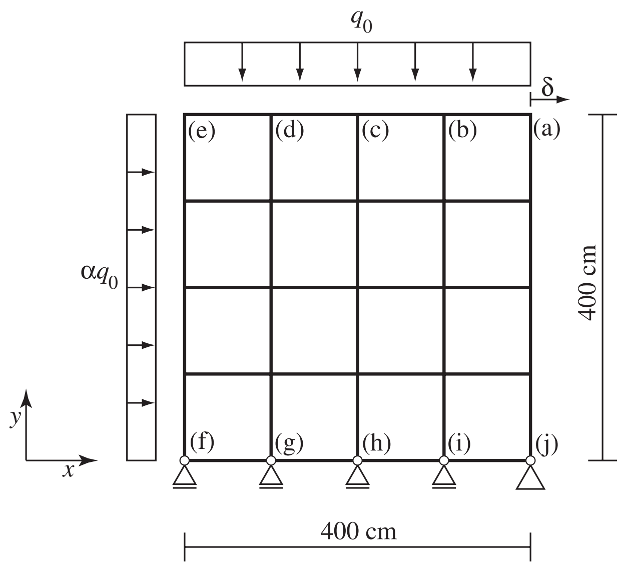

Figure 2: The square wall.

Problem (54) is transformed into the form of Problem (51) as

$$
\left.
\begin{array}{ll}
\min & \displaystyle\sum_{l=1}^{n^{\rm m}} \sum_{i=1}^{n^{\rm g}} \tau_i^l - \underline{\widehat{\boldsymbol{f}}} \cdot \boldsymbol{w} \\
\mathrm{s.t.} & \boldsymbol{T}_{\rm p} \cdot \boldsymbol{w} - \underline{\widehat{\boldsymbol{w}}} \in \mathbf{R}_+^{n_{\rm p}^{\rm d}}, \quad -\boldsymbol{T}_{\rm p} \cdot \boldsymbol{w} + \underline{\widehat{\boldsymbol{w}}} \in \mathbf{R}_+^{n_{\rm p}^{\rm d}}, \\
& \begin{pmatrix} \dfrac{\tau_i^l}{2\widehat{\rho}_i} + 1 \\ \dfrac{\tau_i^l}{2\widehat{\rho}_i} - 1 \\ \boldsymbol{G} \cdot \boldsymbol{\zeta}_i^l \end{pmatrix} \in \mathbf{L}_+^{\widehat{\mu}+2} \quad (i = 1, \dots, n^{\rm g};\ l = 1, \dots, n^{\rm m}), \\
& \mathbf{Mat}(\boldsymbol{\zeta}_i^l) - \mathcal{B}_i \cdot \boldsymbol{T}_{\rm f}^l \cdot \boldsymbol{w} \in \mathcal{S}_+^{\mu} \quad (i = 1, \dots, n^{\rm g};\ l = 1, \dots, n^{\rm m}).
\end{array}
\right\} \qquad (55)
$$

□

6 Examples

Equilibrium configurations are computed for structures consisting of no-tension or no-compression material by using the SDP formulations proposed in Section 5. The SDP problems are solved by using SeDuMi Ver. 1.05 [27], which implements the primal-dual interior-point method for the linear programming problems over symmetric cones [4]. Computation has been carried out on Pentium M (1.5GHz with 1GB memory) with MATLAB Ver. 6.5.1 [22].

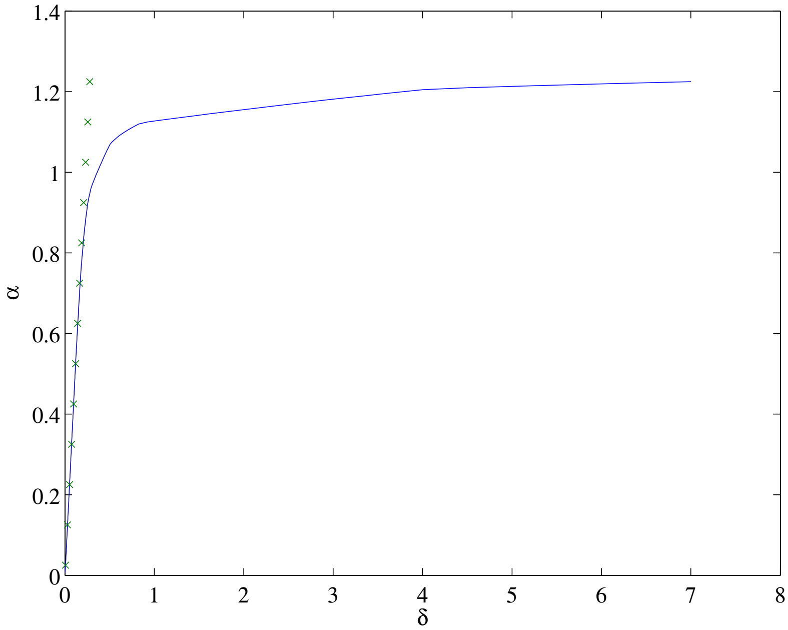

Figure 3: The relation between α and δ (cm) of the square wall; $-$: no-tension material; $\times$: Hooke's material.

6.1 Masonry structure

Consider the masonry square wall illustrated in Fig.2, which consists of the isotropic no-tension material in a state of plane stress. A similar numerical example was investigated by Maier and Nappi [20] with the linear approximation of the admissible region of stresses.

The square wall is discretized into four-node quadrilateral isoparametric finite elements, where $n^{\mathrm{m}} = 16$. The elastic modulus and Poisson's ratio are given as 10^2 GPa and 0.2, respectively. The thickness of the wall is 10 cm. Four sampling points are considered for each element in order to carry out the Gauss integration and evaluate the strain components, i.e., $n^{\mathrm{g}} = 4$. Node (j) is pin-supported, whereas the displacements in the y-direction are constrained at nodes (f)–(i), i.e., $n^{\mathrm{d}} = n^{\mathrm{d}}_{\mathrm{f}} = 44$ and $n^{\mathrm{d}}_{\mathrm{p}} = 0$. Hence, the dimensions of resulting SDP problem (53) are $(\boldsymbol{\zeta}, \boldsymbol{w}, \boldsymbol{\tau}) \in \mathbf{R}^{300}$ and $\mathcal{K} = (\mathbf{L}^5_+ \times \mathcal{S}^2_+)^{64}$.

The constant uniform loading $q_0 = 180$ Ncm^{-1} is applied to the segment (a)–(e) in the negative direction of the y-axis. αq_0 is applied to the segment (e)–(f) in the positive direction of the x-axis with the load factor $\alpha > 0$. The x-component of the displacement of node (a) is denoted by δ. The equilibrium configurations are computed by solving Problem (53) with SeDuMi [27] for various values of α. The obtained results of δ against α are indicated in Fig.3 by the solid curve, where we increase α successively with 245 steps. The mean and standard deviation of CPU time for solving Problem (53) at each step, respectively, are 0.65 sec and 0.21 sec. For comparison purpose, the

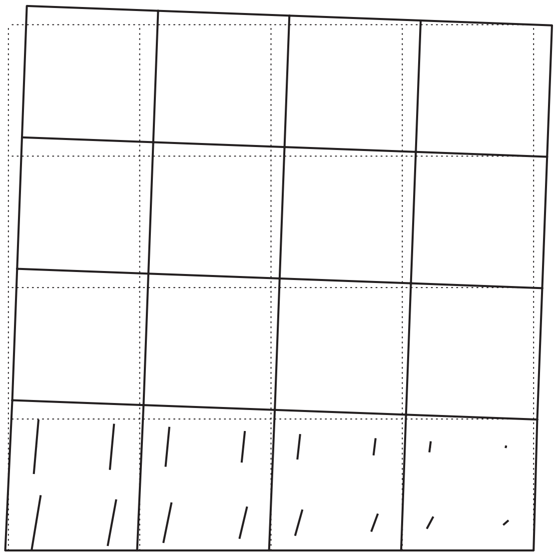

(a) deformed configuration and crack strains (displacements amplified twice)

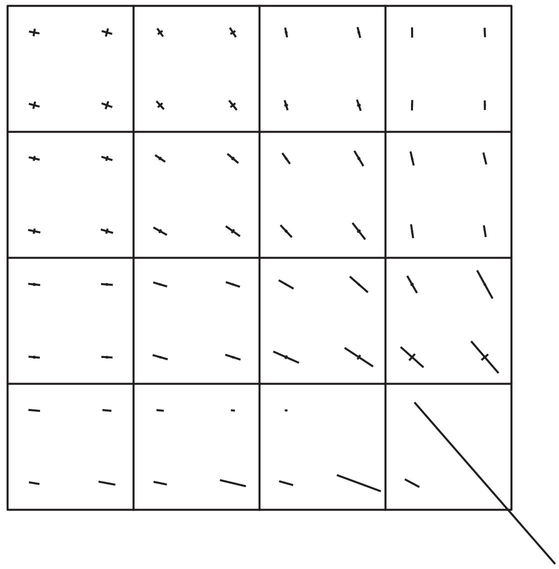

(b) principal stresses

Figure 4: Equilibrium state of the square wall with the no-tension material at $\alpha = 1.225$ and $\delta = 7.001$ cm.

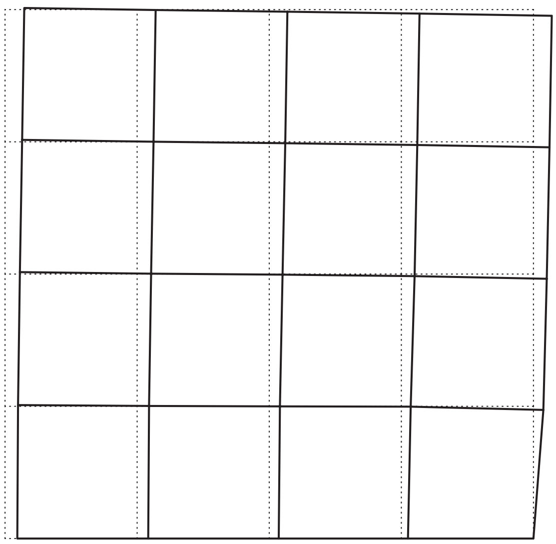

(a) deformed configuration (displacements amplified 50 times)

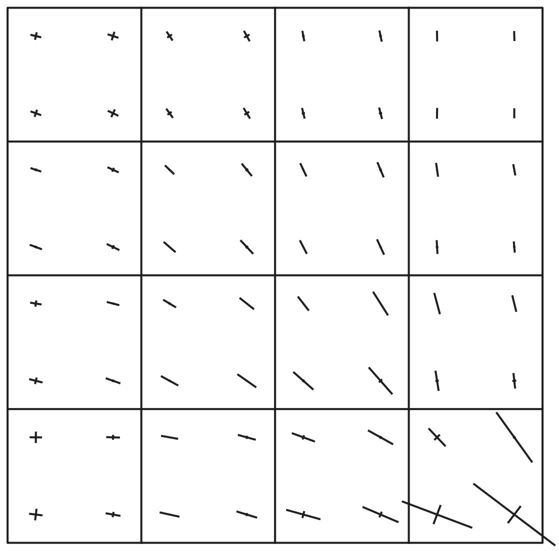

(b) principal stresses

Figure 5: Equilibrium state of the square wall with Hooke's material at $\alpha = 1.225$ and $\delta = 0.278$ cm.

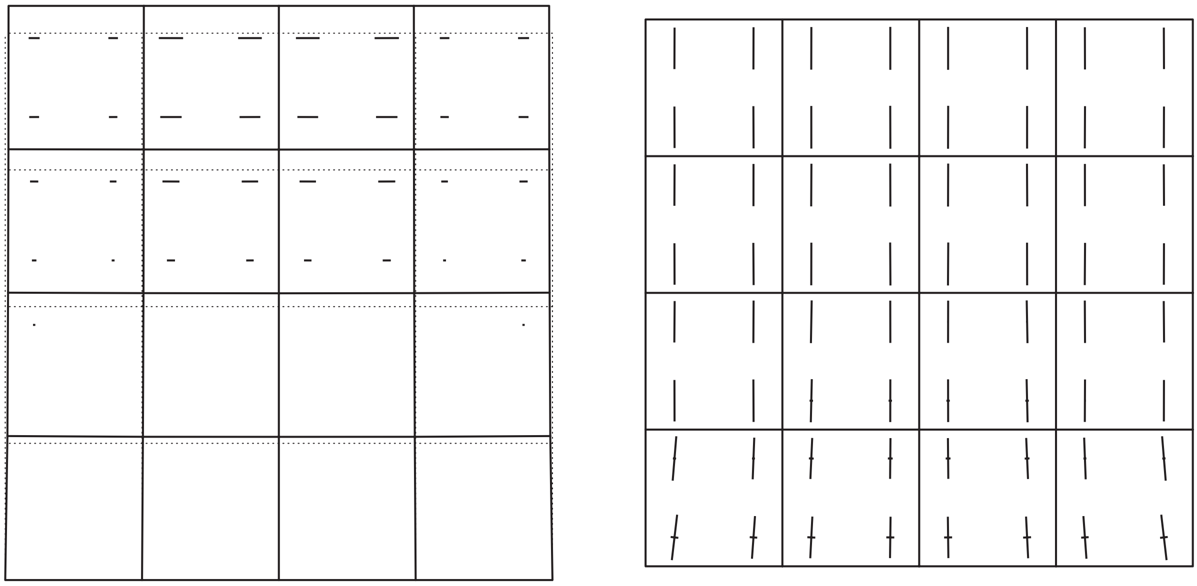

(a) deformed configuration and wrinkle strains

(b) principal stresses

Figure 6: Equilibrium state of the square membrane.

solutions for Hooke's material are also indicated by $\times$. At $\alpha = 1.225$, the obtained configurations of the no-tension material and Hooke's material, respectively, are illustrated in Fig.4 (a) and Fig.5 (a). The principal values and directions of stresses at the Gauss integration points are illustrated in Fig.4 (b) and Fig.5 (b). Here, the solid segments are parallel to the principal axes of stresses, i.e., to the eigenvectors of stress tensors, and the length of each segment is proportional to the modulus of corresponding principal value. Fig.4 (a) also illustrates the principal directions and principal values of $(\boldsymbol{E} - \boldsymbol{Z})$ at the integration points. Hence, smeared cracks are observed in the directions orthogonal to the segments indicated in Fig.4 (a), and the amount of each crack is proportional to the length of corresponding segment. It is observed from Fig.4 that the proposed method finds the equilibrium configuration without any difficulty if many cracks occur in various directions.

6.2 Membrane

Suppose that the square wall illustrated in Fig.2 consists of the no-compression material, where the elastic modulus, Poisson's ratio, and the thickness are 2.5 GPa, 0.2, and 0.4 cm, respectively. The equilibrium configuration is computed based on the SDP formulation (54) of the minimization problem of total potential energy.

Nodes (f)–(j) are pin-supported, i.e., $n^{\mathrm{d}} = 40$, whereas nodes (a)–(e) are subjected to the prescribed displacements of 20 cm in the positive direction of the y-axis, i.e., $n^{\mathrm{d}}_{\mathrm{p}} = 5$ and $n^{\mathrm{d}}_{\mathrm{f}} = 35$. Hence, the dimensions of resulting SDP problem (55) are $(\boldsymbol{\zeta}, \boldsymbol{w}, \boldsymbol{\tau}) \in \mathbf{R}^{296}$ and $\mathcal{K} = \mathbf{R}^{10}_{+} \times (\mathbf{L}^{5}_{+} \times$

$\mathcal{S}_{+}^{2})^{64}$.

No external forces are applied, i.e., $\hat{\boldsymbol{f}} = \mathbf{0}$. The obtained equilibrium configuration is illustrated in Fig.6 (a), where the CPU time of 0.46 sec is required by SeDuMi [27]. Fig.6 (a) also illustrates the principal directions and values of $(\boldsymbol{Z} - \boldsymbol{E})$ at the integration points, where the direction of each segment is orthogonal to wrinkling pattern, and the length of each segment is proportional to the amount of wrinkle. The corresponding principal stresses are illustrated in Fig.6 (b). It is observed from Fig.6 (a) that the presented method can find the equilibrium configuration, as well as the wrinkling pattern, without any difficulty even if many elements are wrinkling.

7 Conclusions

A unified approach based on SDP has been proposed for finding equilibrium configurations of structures consisting of no-tension or no-compression isotropic non-dissipative material under the assumption of small deformations.

A convex variational problem has been formulated which gives the same optimizer as that of the minimization problem of total potential energy. By applying the conventional displacement-based finite-element discretization procedure, the proposed variational problem can be discretized into the SDP problem. We can obtain an equilibrium configuration an optimal solution of the presented SDP problem by using the primal-dual interior-point method.

The presented SDP formulation is independent of the fact that the structure is two- or three-dimensional. Moreover, the formulation includes no a priori knowledge on the stress states. Therefore this method does not involve any processes of trial-and-error even if the structure has complicated patterns of smeared cracks or wrinkling. It is guaranteed that the number of arithmetic operations required by this method is bounded by a polynomial of the size of problem. Numerical examples have shown the effectiveness of this method for the cases of many cracks or wrinkles occur at equilibrium configurations.

Besides these advantages, SDP can be solved efficiently by using the well-developed softwares based on the primal-dual interior-point method. Hence, no effort is required to develop any analysis software, and we only have to prepare the constant matrices and vectors defining the SDP problems. Since our finite-element discretization is based on the usual displacement-based finite element methods, it is easy to construct these matrices and vectors by utilizing the conventional softwares of finite element method.

References

[1] **Alfano, G.; Rosati, L.; Valoroso, V.:** A numerical strategy for finite element analysis of no-tension materials. International Journal for Numerical Methods in Engineering 48 (2000) 317–350.

[2] **Alizadeh, F.; Haeberly, J.-P.A.; Overton, M.L.:** Complementarity and nondegeneracy in semidefinite programming. Mathematical Programming 77 (1997) 111–128

[3] **Atai, A.A.; Steigmann, D.J.:** Coupled deformations of elastic curves and surfaces. International Journal of Solids and Structures 35 (1998) 1915–1952

[4] **Ben-Tal, A.; Nemirovski, A.:** Lectures on Modern Convex Optimization: Analysis, Algorithms, and Engineering Applications. SIAM, Philadelphia, Pennsylvania 2001

[5] **Berto, L.; Saetta, A.; Scotta, R.; Vitaliani, R.:** An orthotropic damage model for masonry structures. International Journal for Numerical Methods in Engineering 55 (2002) 127–157

[6] **Bull, J.W. (ed.):** Computational Modeling of Masonry, Brickwork and Blockwork Structures. Saxe-Coburg Publications, Stirling, UK 2001

[7] **Cuomo, M.; Ventura, G.:** A complementary energy formulation of no tension masonry-like solids. Computer Methods in Applied Mechanics and Engineering 189 (2000) 313–339

[8] **de Falco, A.; Lucchesi, M.:** Stability of columns with no tension strength and bounded compressive strength and deformability. Part I: large eccentricity. International Journal of Solids and Structures 39 (2002) 6191–6210

[9] **Epstein, M.; Forcinito, M.A.:** Anisotropic membrane wrinkling: theory and analysis. International Journal of Solids and Structures 38 (2001) 5253–5272

[10] **Formica, G.; Sansalone, V.; Casciaro, R.:** A mixed solution strategy for the nonlinear analysis of brick masonry walls. Computer Methods in Applied Mechanics and Engineering 191 (2002) 5847–5876

[11] **Giaquinta, M.; Giusti, E.:** Researches on the equilibrium of masonry structures. Archive for Rational Mechanics and Analysis 88 (1985) 359–392

[12] **Helmberg, C.;** Semidefinite programming for combinatorial optimization. ZIB-Report ZR-00-34, Konrad-Zuse-Zentrum Berlin, 2000

[13] **Jarre, F.:** Some aspects of nonlinear semidefinite programming. System Modeling and Optimization XX: Ifip Tc7 20th Conference on System Modeling and Optimization, Edited by E.W. Sachs and R. Tichatschke, Kluwer Academic Publishers, pp. 55–69, 2003

[14] **Kanno, Y.; Martins, J.A.C.; Pinto da Costa, A.:** Three-dimensional quasi-static frictional contact by using second-order cone linear complementarity problem. BGE Research Report 04-01, Building Geoenvironment Engineering Laboratory, Kyoto University, Japan, February 2004

[15] **Kanno, Y.; Ohsaki, M.; Ito, J.:** Large-deformation and friction analysis of nonlinear elastic cable networks by second-order cone programming. International Journal for Numerical Methods in Engineering 55 (2002) 1079–1114

[16] **Kanno, Y.; Ohsaki, M.; Katoh, N.:** Sequential semidefinite programming for optimization of framed structures under multimodal buckling constraints. International Journal of Structural Stability and Dynamics 1 (2001) 585–602

[17] **Kanzow, C.; Nagel, C.; Fukushima, M.:** Successive linearization methods for nonlinear semidefinite programs. Technical Report 2003-011, Department of Applied Mathematics and Physics, Kyoto University, August 2003

[18] **Kojima, M.; Shindoh, S.; Hara, S.:** Interior-point methods for the monotone semidefinite linear complementarity problems. SIAM Journal on Optimization 7 (1997) 86–125

[19] **Lu, K.; Accorsi, M.; Leonard, J.:** Finite element analysis of membrane wrinkling. International Journal for Numerical Methods in Engineering 50 (2001) 1017–1038

[20] **Maier, G.; Nappi, A.:** A theory of no-tension discretized structural systems. Engineering Structures 12 (1990) 227–234

[21] **Marfia, S.; Sacco, E.:** Modeling of reinforced masonry elements. International Journal of Solids and Structures 38 (2001) 4177–4198

[22] **The MathWorks, Inc.:** Using MATLAB. The MathWorks, Inc., Natick, Massachusetts 1999

[23] **Ohsaki, M.; Fujisawa, K.; Katoh, N.; Kanno, Y.:** Semi-definite programming for topology optimization of trusses under multiple eigenvalue constraints. Computer Methods in Applied Mechanics and Engineering 80 (1999) 203–217

[24] **Padovani, C.; Pasquineli, G.; Zani, N.:** A numerical method for solving equilibrium problems of no-tension solids subjected to thermal loads. Computer Methods in Applied Mechanics and Engineering 190 (2000) 55–73

[25] **Pipkin, A.C.:** Relaxed energy densities for small deformations of membranes. IMA Journal of Applied Mathematics 50 (1993) 225–237

[26] **Rockafellar, R.T.:** Convex Analysis. Princeton University Press, Princeton, New Jersey 1970

[27] **Sturm, J. F.,** Using SeDuMi 1.02, a MATLAB toolbox for optimization over symmetric cones. Optimization Methods and Software 11/12 (1999) 625–653

[28] **Todd, M.J.; Toh, K.C.; Tütüncü, R.H.;** On the Nesterov-Todd direction in semidefinite programming. SIAM Journal on Optimization 8 (1998) 769–796

[29] **Wolkowicz, H.; Saigal, R.; Vandenberghe, L. (eds.):** Handbook of Semidefinite Programming — Theory, Algorithms, and Applications. Kluwer Academic Publishers, Dordrecht, The Netherlands 2000

[30] **Zienkiewicz, O.C.; Taylor, R.L.:** The Finite Element Method (4th ed.). McGraw-Hill, London, UK 1987/89